Modeling of an IGC Experiment to Analyze Ternary Polymer–Solvent Systems

Peter K. Davis, J. Larry Duda, and Ronald P. Danner
Center for the Study of Polymer Solvent Systems, Dept. of Chemical Engineering, The Pennsylvania State University, University Park, PA 16802

DOI 10.1002/aic.10551
Published online September 13, 2005 in Wiley InterScience (www.interscience.wiley.com).

A variation of the capillary column inverse gas chromatography (IGC) experiment is proposed to measure the thermodynamics and diffusion coefficients in ternary polymer–solvent–solvent systems, and a theoretical model has been developed for this proposed experiment. The model has been derived to include both main and mutual cross-diffusion coefficients. Ternary vapor–liquid equilibria was represented by a coefficient matrix of the isotherm tangents. The governing equations of the model were uncoupled and solved using both an analytical Laplace transform technique and a numerical finite-difference technique. Solution of the model shows that in the presence of strong cross-diffusion and thermodynamic coefficients, unusual chromatographic behavior can be observed, suggesting that IGC can be a useful technique for measuring thermodynamic and mass-transport properties of ternary polymer–solvent–solvent systems. © 2005 American Institute of Chemical Engineers *AIChE J,* 51: 2930–2941, 2005
Keywords: inverse gas chromatography (IGC), multicomponent diffusion and thermodynamics, polymer–solvent systems, modeling

Introduction

Capillary column inverse gas chromatography (CCIGC) has proven to be a useful experimental technique to measure thermodynamic and mass-transport properties in polymer–solvent systems.[1-5] In CCIGC, a thin film of polymer is coated on the inside of a capillary wall. An inert carrier gas transports a small pulse of solvent through the column and a detector measures the elution of solvent from the column. Because the solvent absorbs and diffuses through the thin polymer film, the solvent elution can be related to the partition coefficient and diffusion coefficient by comparison to a theoretical model. Capillary columns have a major advantage over packed columns because the polymer coating thickness is much more uniform, thus allowing accurate measurement of diffusion coefficients. Inverse gas chromatography has been used in the past to measure diffusion coefficients for binary and pseudobinary polymer–solvent systems. Danner et al.[5] used finite-concentration CCIGC to measure effective diffusion coefficients of toluene and methanol in the PVAc–methanol–toluene system.

A true ternary polymer–solvent–solvent system has a matrix of four mutual diffusion coefficients that govern mass transport

$$[D_p] = \begin{bmatrix} D_{p11} & D_{p12} \\ D_{p21} & D_{p22} \end{bmatrix} \tag{1}$$

The subscripts indicate solvent 1 and solvent 2. The D_{p11} and D_{p22} are referred to as the *main terms* of the diffusion coefficient matrix and D_{p12} and D_{p21} are the *cross terms*. The diffusive flux of each solvent, $j_i^{\neq}$, in such a system can be defined in terms of these diffusion coefficients relative to the system's volume average velocity

Correspondence concerning this article should be addressed to J. L. Duda at jld@psu.edu.

$$j_1^{\neq} = -D_{p11}\nabla\rho_1 - D_{p12}\nabla\rho_2 \quad (2)$$

$$j_2^{\neq} = -D_{p21}\nabla\rho_1 - D_{p22}\nabla\rho_2 \quad (3)$$

Here, $\nabla\rho_i$ is the gradient in mass concentration of solvent i.

Finite-concentration IGC has been used by Joffrion and Glover[6] and Tsotsis et al.[7] to measure ternary-phase equilibria and effective binary diffusivities, but not the cross-diffusivities. Diffusion coefficients in polymer–solvent systems are usually measured by gravimetric-type experiments. Binary gravimetric experiments are fairly simple. The single binary diffusion coefficient is determined from the time needed to equilibrate a polymer sample with the vapor of solvent. Gravimetric experiments proceed by measuring the weight gain of the polymer vs. time. There are several sorption experiments that rely on this type of measurement, although these experiments fail for ternary experiments because the weight gain of the sample arises from sorption of both solvents. Thus, it is not possible to determine how much of each solvent is in the polymer vs. time. Furthermore, the vapor is no longer pure, and the composition of this phase must also be known as a function of time. A modified quartz spring gravimetric experiment has been used to measure solubility (not diffusion) of two solvents in a polymer.[8,9]

Although gravimetric experiments are quite common for measuring diffusion coefficients, they are not the only available techniques. Infrared spectroscopy has been used to measure the cross-diffusion coefficients in the PIB–MEK–toluene system.[10] Drying experiments are another possibility to measure ternary diffusion coefficients.[11] In such an experiment, a polymer–solvent–solvent solution is devolatilized in a convective oven. Measurement of the effluent solvent concentration in the vapor phase can be used to determine the polymer solution weight loss arising from both solvents vs. time. Such an experiment relies on extensive modeling because mass and heat transfer occur in both the vapor and polymer phases. In addition, the experiment is conducted over extremely wide ranges of solvent concentration in the polymer phase. Thus, the experiment relies heavily on a model for the concentration dependency of the diffusion coefficients. Such models do exist, but have not been tested because of the absence of any ternary diffusion data.[12,13] Inverse gas chromatography has a major advantage over drying because experiments are conducted at a single concentration (usually at infinite dilution). However, experiments can be conducted at finite concentrations as shown by several investigators.[5,6,14-16]

In this communication, a new CCIGC experiment is proposed to measure the four member diffusion coefficient matrix and vapor–liquid equilibria at finite concentrations in ternary polymer–solvent–solvent solutions. Analysis of such an experiment requires a model that describes the complex diffusion process in the column. A new CCIGC model has been developed capable of analyzing ternary CCIGC data.

Proposed Experimental Procedure

The proposed experiment is an extension of that used by Danner et al.[5] to measure properties of pseudobinary systems. A diagram of this new experimental setup is shown in Figure 1.

A quartz capillary column is coated with a thin film of the polymer of interest and a ternary mixture of an inert carrier gas and vapor of the two solvents is continuously passed through the column. The vapor composition is controlled by the temperature of the two saturators containing each of the pure solvents. The effluent streams from the saturators are then mixed and sent through the column giving a ternary vapor mixture of constant concentration. When equilibrium is attained, a small amount of one of the solvents is injected into the column. This perturbation of solvent travels through the column and interacts with the polymer–solvent–solvent mixture. A suitable detector measures the vapor concentration of each solvent at the exit of the column. The detector must be capable of distinguishing between each solvent while they are eluding simultaneously. The common thermal conductivity detector (TCD) or flame ionization detector (FID) will not work because these will give an average reading for both solvents. Because the injection perturbs the vapor composition of both solvents, the experiment will produce elution profiles for both solvents. Analysis of both elution profiles gives information about the thermodynamics and diffusion coefficients of the ternary system.

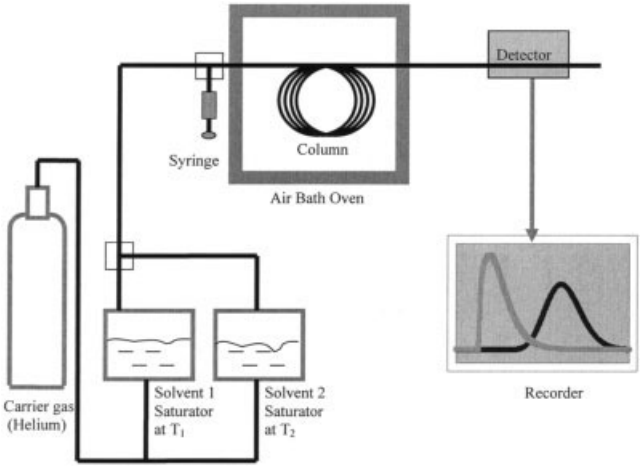

Figure 1. Proposed experimental setup for a ternary CCIGC experiment.

Model for Ternary CCIGC Experiments

The original CCIGC model was developed by Macris[1] for binary polymer–solvent systems at infinite dilution. The vapor phase was pure carrier gas containing a small solvent concentration from the injection. Here, this model is extended to ternary polymer–solvent–solvent systems at finite solvent gas concentrations. A diagram of the process to be modeled is show in Figure 2.

In the derivation of the model, the following assumptions are made:

(1) The entire system is isothermal.

(2) The pressure drop in the column is insignificant.

(3) The polymer coating thickness is much smaller than the column radius.

(4) Gas-phase diffusion is fast enough to keep the solvent radially well mixed, making Taylor dispersion insignificant compared to conventional axial dispersion.

(5) The polymer-phase diffusion coefficients are constant

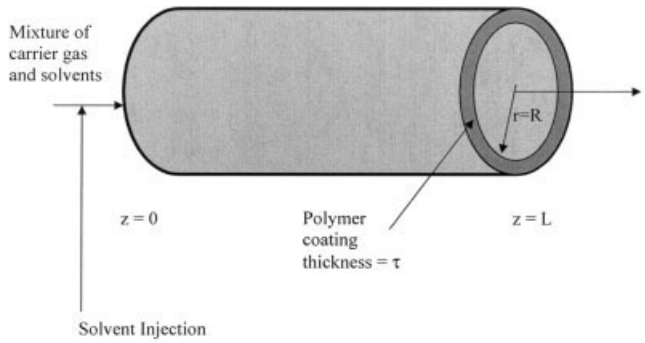

Figure 2. Ternary CCIGC experiment.

within the small concentration range of the solvent perturbations.

(6) The vapor-phase diffusion coefficients are constant and the vapor-phase cross-diffusion coefficients are negligible.

(7) The thermodynamics of bulk absorption can be described by a coefficient matrix of the isotherm tangent slopes. These coefficients are constant over the small concentration range of the perturbation.

(8) The polymer film has a uniform thickness through the entire column.

(9) The only significant diffusion in the polymer phase occurs in the radial direction.

(10) The carrier gas is insoluble in the polymer and does not adsorb on any surfaces.

(11) Surface adsorption by the solvents is negligible.

(12) No chemical reactions occur.

(13) The partial molar volume of the solvents in the polymer is constant.

(14) Swelling of the polymer is insignificant over the concentration range of the perturbation.

(15) The solvent injection can be modeled by a Dirac delta function.

Based on assumption (2), the pressure in the column is constant. Because the total pressure in the column is never much greater than atmospheric, it will be assumed that the ideal gas law applies. An ideal gas at constant temperature and total pressure has a constant molar density C^{molar}

$$C^{\text{molar}} = \frac{C_1}{M_1} + \frac{C_2}{M_2} + \frac{C_3}{M_3} \qquad \text{(constant)} \tag{4}$$

Here, C_i is the mass concentration of each species in the gas phase and M_i is the molecular weight of each species. The subscripts define the following species in the vapor: 1 = solvent 1, 2 = solvent 2, and 3 = inert carrier gas. Furthermore, because the solvent perturbation is small compared to the overall concentration, the overall mass density (C) of the gas is approximately constant

$$C = C_1 + C_2 + C_3 \approx \text{constant} \tag{5}$$

Under this approximation, the species continuity equations in the gas phase can be expressed relative to the mass average velocity (V)

$$\frac{\partial C_1}{\partial t} + \frac{\partial}{\partial z}(C_1 V) = D_{g11}\frac{\partial^2 C_1}{\partial z^2} + \frac{2}{R}\left(D_{p11}\left.\frac{\partial \rho_1}{\partial r}\right|_{r=R} + D_{p12}\left.\frac{\partial \rho_2}{\partial r}\right|_{r=R}\right) \tag{6}$$

$$\frac{\partial C_2}{\partial t} + \frac{\partial}{\partial z}(C_2 V) = D_{g22}\frac{\partial^2 C_2}{\partial z^2} + \frac{2}{R}\left(D_{p21}\left.\frac{\partial \rho_1}{\partial r}\right|_{r=R} + D_{p22}\left.\frac{\partial \rho_2}{\partial r}\right|_{r=R}\right) \tag{7}$$

$$\frac{\partial C_3}{\partial t} + \frac{\partial}{\partial z}(C_3 V) = -\left(D_{g11}\frac{\partial^2 C_1}{\partial z^2} + D_{g22}\frac{\partial^2 C_2}{\partial z^2}\right) \tag{8}$$

Here, ρ_i represents the mass concentrations of the solvents in the polymer phase. In the polymer phase, the subscript 1 denotes solvent 1 and 2 represents solvent 2. In this formulation, the cross-diffusion coefficients in the gas phase are assumed to be negligible. The appropriate boundary conditions are

$$t = 0 \qquad \begin{bmatrix} C_1 \\ C_2 \\ C_3 \end{bmatrix} = \begin{bmatrix} C_{b1} \\ C_{b2} \\ C_{b3} \end{bmatrix} \qquad V = V_0 \tag{9}$$

$$z = 0 \qquad \begin{bmatrix} C_1 \\ C_2 \\ C_3 \end{bmatrix} = \begin{bmatrix} \delta(t)C_{01} + C_{b1} \\ \delta(t)C_{02} + C_{b2} \\ \delta(t)C_{03} + C_{b3} \end{bmatrix} \tag{10}$$

$$z = \infty \qquad \begin{bmatrix} C_1 \\ C_2 \\ C_3 \end{bmatrix} = \begin{bmatrix} C_{b1} \\ C_{b2} \\ C_{b3} \end{bmatrix} \qquad V = V_0 \tag{11}$$

Here, C_{0i} is the strength of the pulse of species i and C_{bi} is the background (plateau) concentration of species i.

Assuming that the polymer thickness is much smaller than the column radius, the two solvent species continuity equations in matrix notation for the polymer phase are

$$\frac{\partial}{\partial t}\begin{bmatrix} \rho_1 \\ \rho_2 \end{bmatrix} = \begin{bmatrix} D_{p11} & D_{p12} \\ D_{p21} & D_{p22} \end{bmatrix}\frac{\partial^2}{\partial r^2}\begin{bmatrix} \rho_1 \\ \rho_2 \end{bmatrix} \tag{12}$$

$$t = 0 \qquad \begin{bmatrix} \rho_1 \\ \rho_2 \end{bmatrix} = \begin{bmatrix} \rho_{b1} \\ \rho_{b2} \end{bmatrix} = \begin{bmatrix} \int_0^{C_{b1}} K_{p11}dC_1 + \int_0^{C_{b2}} K_{p12}dC_2 \\ \int_0^{C_{b1}} K_{p21}dC_1 + \int_0^{C_{b2}} K_{p22}dC_2 \end{bmatrix} \tag{13}$$

$$r = R \qquad \begin{bmatrix} \rho_1 \\ \rho_2 \end{bmatrix} = \begin{bmatrix} \int_0^{C_1} K_{p11}dC_1 + \int_0^{C_2} K_{p12}dC_2 \\ \int_0^{C_1} K_{p21}dC_1 + \int_0^{C_2} K_{p22}dC_2 \end{bmatrix} \tag{14}$$

$$r = r + \tau \qquad \frac{\partial}{\partial r}\begin{bmatrix}\rho_1\\ \rho_2\end{bmatrix} = \begin{bmatrix}0\\ 0\end{bmatrix} \tag{15}$$

Here K_{pij} is the slope of the isotherm tangent and ρ_{bi} is the background (plateau) concentration of species i.

The diffusive fluxes are defined with respect to the volume average velocity in the polymer phase. Equations 6, 7, 8, and 12 constitute five coupled partial differential equations that must be solved to model the elution of the two solvents from the column. These equations were uncoupled using a coordinate transformation[17] and were solved using the technique of Laplace transforms. The details of the solution are in Appendix A. In the solution, it is shown that the solvent concentration in the gas phase at the detector can be expressed in the Laplace domain

$$\hat{Y}_i = H_i \exp\left\{\frac{1}{2\gamma_i} - \sqrt{\frac{1}{4\gamma_i^2} + \psi_i(s)}\right\} \tag{16}$$

Here, $\hat{Y}_i$ is a pseudo-Laplace variable for the gas concentration of solvent i at the detector. H_i, γ_i, and $\psi_i(s)$ are vectors of dimensionless parameters. Analytical inversion of Eq. 16 into the time domain is not possible, so numerical inversion was used to solve the model by a Fast Fourier Transform (FFT) algorithm.

Model Predictions for Ternary CCIGC Experiments

The purpose of deriving this model is to permit analysis of experimental ternary elution profiles with the intent of determining the matrix of diffusion and thermodynamic coefficients. The D_{pii} and K_{pii} are often referred to as the *main terms*, whereas D_{pij} and K_{pij} are referred to as the *cross terms* in the coefficient matrices.

The aim here is to measure all four diffusion and thermodynamic coefficients. It is questionable that all eight unique parameters can be obtained from the elution profiles of a single CCIGC experiment. For this reason, experiments should be conducted with two different columns. The first column should be designed such that there is negligible diffusion resistance in the polymer phase. This is accomplished by coating a very long column with a sufficiently thin polymer coating. Because there will be negligible mass transfer resistance, experiments with this column will produce symmetric elution profiles that are independent of the diffusion coefficients. These elution profiles can be uniquely related to the thermodynamic coefficients. Once the thermodynamic coefficients are known, a second, shorter column should be made with a thicker coating to give significant diffusion resistance. Experiments on this column will give asymmetric elution profiles that can be used to obtain a unique set of four mutual diffusion coefficients.

Diffusion coefficient sensitivity

Experiments on the short, thick column will produce elution profiles that depend on the diffusion coefficients. It is possible that mass transport in the ternary system can be described using only the main diffusion coefficients (cross-diffusion coefficients equal to zero). This effectively corresponds to two pseudobinary diffusion processes because the two solvents will diffuse independent of each other. Although the proposed experiment is capable of measuring such pseudobinary diffusion coefficients, it is also possible that both main and cross-diffusivities are needed to accurately describe the mass-transport process. In such a case, the elution profiles of the two solvents must provide information about all four diffusion coefficients. To demonstrate the effect of the cross-diffusion coefficients on the elution profile, the model described above was solved over varying ranges of the cross-diffusion coefficients. Nominal values of the other parameters were used in the simulations. The cross thermodynamic coefficients were assumed to be zero. The results of the simulations are shown in Figures 3, 4, and 5. The dimensionless parameters for the simulations are given in Table 1. In each of the figures, a different value of the ratio of the cross-diffusion coefficient to the main diffusion coefficient for both of the two solvents was used.

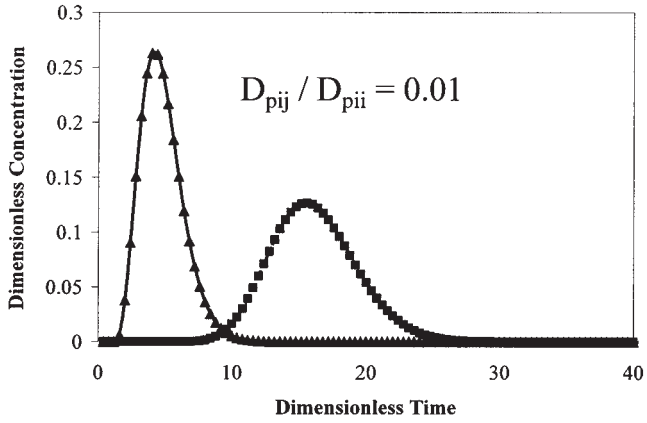

Figure 3. Simulation of a ternary CCIGC experiment.

Solid line is ternary model prediction for solvent 1 and dotted line is that for solvent 2. Symbols indicate ternary model simulation for insignificant cross terms ($D_{pij} = 0$): solvent 1 (▲), solvent 2 (■).

In Figure 3, the cross-diffusion coefficients are 100 times smaller than the main diffusion coefficients. Under such conditions, the cross-diffusion coefficients make essentially no contribution to the shape of the elution profiles. There was also only a negligible difference when the cross terms were 75% smaller than the main terms (not shown). In these cases, mass transport in the ternary system can be accurately represented as two pseudobinary systems because diffusion of the two solvents can be described by just the main diffusion coefficients.

Table 1. Values of the Dimensionless Groups for the Simulations in Figures 3, 4, and 5*

Parameter	Figure 3	Figure 4	Figure 5
α_{11}	0.53	0.53	0.53
α_{22}	0.13	0.13	0.13
$\alpha_{12} = \alpha_{21}$	∞	∞	∞
β_{11}	1.0	1.0	1.0
β_{12}	10.0	1.1	1.01
β_{21}	10.0	1.1	1.01
β_{22}	1.0	1.0	1.0
$\gamma_1 = \gamma_2$	1.0×10^{-4}	1.0×10^{-4}	1.0×10^{-4}
λ	1.0	1.0	1.0

*Dimensionless group definitions are given in Appendix A.

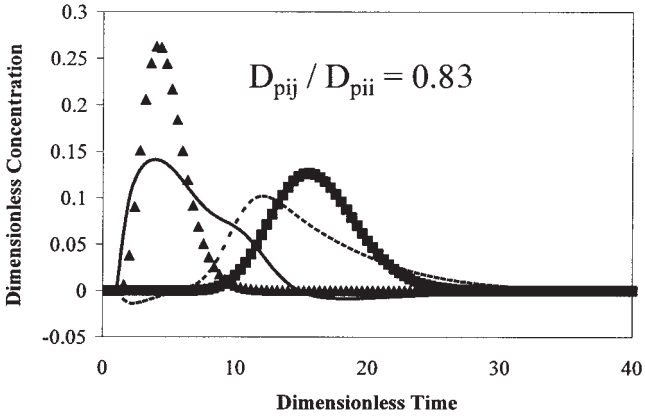

Figure 4. Simulation of a ternary CCIGC experiment.

Solid line is ternary model prediction for solvent 1 and dotted line is that for solvent 2. Symbols indicate ternary model simulation for insignificant cross terms ($D_{pij} = 0$): solvent 1 (▲), solvent 2 (■).

However, the diffusion cross terms used in Figures 4 and 5 definitely give elution profiles different from those obtained without cross terms. In these cases, it is not possible to represent the ternary diffusion processes as two pseudobinary systems. Interestingly, the elution profiles give very unusual behavior in the presence of significant diffusion cross terms. Multiple peaks and solvent concentrations dipping below their baseline are observed under such conditions. This unique behavior can be quite useful when trying to determine the significance of the cross-diffusion coefficients in polymer–solvent systems. If the cross-diffusion coefficients are negligible, single peaks and positive *dimensionless* concentrations will be observed in a CCIGC experiment. If multiple peaks and negative *dimensionless* concentrations are observed from the IGC, then the cross-diffusion coefficients are significant and can be measured. Performing experiments at different solvent concentrations can give the concentration dependency of both main and cross-diffusion coefficients in ternary polymer–solvent systems.

The diffusion coefficients in the matrix are not independent

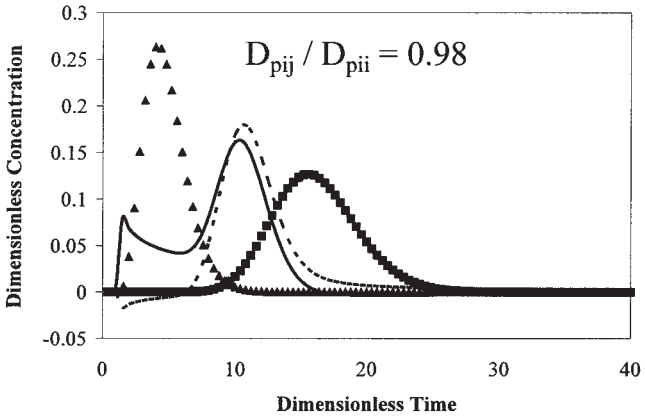

Figure 5. Simulation of a ternary CCIGC experiment.

Solid line is ternary model prediction for solvent 1 and dotted line is that for solvent 2. Symbols indicate ternary model simulation for insignificant cross terms ($D_{pij} = 0$): solvent 1 (▲), solvent 2 (■).

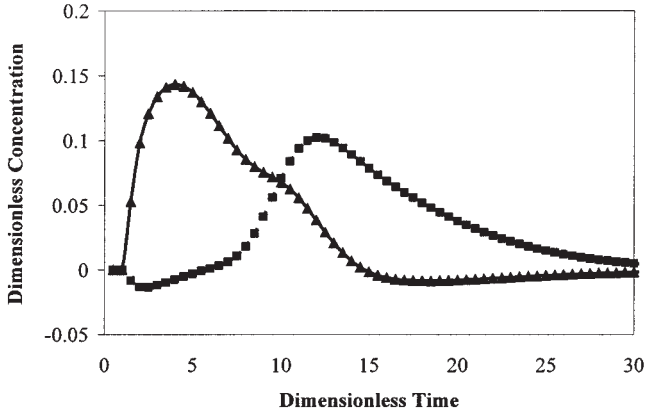

Figure 6. Numerical simulations to determine the effect of axial dispersion on the elution profile.

Solid line is analytical model prediction for solvent 1 and dotted line is that for solvent 2 when $D_{g11} = D_{g22}$. Symbols: solvent 1 (▲), and solvent 2 (■), indicate numerical model solution when $D_{g22} = 10D_{g11}$. All other parameters were the same as those used in Figure 4.

of each other. They are constrained by material balances, the Onsager reciprocal relationships, and thermodynamic stability. The Onsager relationships and thermodynamic stability specify that the diffusion coefficient matrix has real-positive eigenvalues.[18] For a ternary system, the necessary constraint to ensure this is

$$D_{p11} + D_{p22} > 0$$

$$D_{p11}D_{p22} - D_{p12}D_{p21} \geq 0$$

$$(D_{p11} + D_{p22})^2 \geq (D_{p11}D_{p22} - D_{p12}D_{p21}) \qquad (17)$$

In all simulations, these expressions were obeyed and no material balances were violated. Material balance violation can be detected by negative *dimensional* concentrations.[19] Negative concentrations can be obtained by solving the continuity equations with unrealistic diffusion coefficients. Although the continuity equations can be mathematically satisfied with negative concentrations, a negative mass cannot physically exist. Thus, any negative concentrations violate material balance constraints. In these simulations, no negative concentrations were obtained.

Numerical solution

To this point, model simulations were obtained from the analytical Laplace domain solution. A numerical solution was also developed for the model based on an implicit finite-difference method. The numerical model is quite useful because it can be used to verify some of the assumptions needed for the analytical solution. For example, in the analytical solution (see Appendix A), it was assumed that the gas-phase diffusion coefficient matrix was symmetrical ($D_{g11} = D_{g22}$). It was argued that this assumption had no bearing on the elution profiles of the solvents. To test this argument, the numerical solution was generated for $D_{g11} = D_{g22}$ and for $D_{g22} = 10 \times D_{g11}$. The results of the simulation are shown in Figure 6. Even

when the gas-phase diffusion coefficients are different by a factor of 10, the elution profiles are still the same. This verifies the assumption of a symmetric D_g matrix. More details for the numerical solution can be found in Appendix B.

Parameter Estimation

In the proposed experiment, the diffusion coefficient and thermodynamic coefficient matrices will be obtained from the elution profiles of the two solvents. Eight unknown parameters are needed to completely describe these elution profiles. As mentioned, experiments should be carried out using two different columns. The first column should be designed to give an insignificant amount of diffusion resistance in the polymer. Experiments on this column can be used to obtain the thermodynamic coefficients K_{ij}. As described, these are the tangents to the isotherm planes and, although constant during any experiment, they will vary with bulk composition changes. After a number of K_{ij} with sufficient proximity in concentration have been measured, the actual bulk solubilities can be obtained by numerical integration according to Eq. 13 subject to the initial conditions ($C_i = 0$, $\rho_i = 0$).

Experiments on a second, shorter, thicker column should then be used to obtain the diffusion coefficients. Inverse gas chromatography parameter estimation is usually carried out by moment analysis.[1-4] In a binary experiment, the first and second moments can be related to the partition and diffusion coefficient, respectively. This procedure cannot be used directly for ternary analysis because there are more parameters than moments. In addition, the complex Laplace domain expression for Y_i makes the analytical expressions for the moments difficult to obtain. Thus, it is proposed that parameter estimation proceed by Fourier or time domain fitting. In this procedure, the parameters are adjusted such that the experimental elution profiles match the model elution profiles for each solvent. This procedure was first introduced by Pawlisch[2] and used by other investigators for binary systems.[4,5,20,21] In binary experiments, the partition and diffusion coefficient are adjustable parameters used to match the experimental elution to that of the binary model.

Caution must be exercised when measuring the diffusion coefficients at finite concentrations arising from variation in the coating thickness τ. As the solvents swell the polymer coating, the film thickness will increase. In general, this will lead to an underestimation of the diffusion coefficients. During any particular experiment, the small solvent perturbation does not significantly change the coating thickness, but as the bulk concentration changes from experiment to experiment, swelling will become important. However, because the experiments on the column with insignificant diffusion resistance give the thermodynamics of the polymer–solvent–solvent system, this swelling can be predicted and accurate diffusion coefficients can be obtained.

Summary and Conclusions

A new capillary column inverse gas chromatography experiment has been proposed to measure the four member diffusion coefficient matrix and the vapor–liquid equilibrium in ternary polymer–solvent–solvent systems. The proposed experiment is capable of measuring the diffusion and partition coefficients over wide ranges of solvent concentration. The uniqueness and power of this technique is that an experiment is conducted by measuring a small solvent perturbation around a fixed composition. Thus, experiments are performed at a given solvent concentration such that the diffusion and thermodynamic coefficients can be considered constant. A model has been developed that describes the complex diffusion process in the column. Both analytical and numerical solutions have been obtained. Simulation of the proposed experiment indicates that CCIGC is quite sensitive to the cross-diffusion coefficients when they are of comparable order to the main terms. This sensitivity makes CCIGC a promising technique to measure the values of all four diffusion coefficients and the true vapor–liquid equilibrium in ternary polymer–solvent–solvent systems.

Notation

ρ_i = mass concentration of species i in the polymer phase, kg/m^3
ρ_{bi} = background mass concentration of species i in the polymer phase, kg/m^3
C = mass density of the vapor phase, kg/m^3
C_i = mass concentration of species i in the vapor phase, kg/m^3
C_{bi} = background mass concentration of solvent i in the vapor phase, kg/m^3
C_{0i} = strength of the solvent pulse (kg-s/m^3) for species i
D_{pij} = mutual binary diffusion coefficient matrix for the polymer phase, m^2/s
D_{gij} = mutual binary diffusion coefficient matrix for the gas phase, m^2/s
K_{pij} = dimensionless coefficient matrix (isotherm tangent slope) describing the thermodynamics between the gas and polymer phases
L = column length, m
M_i = molecular weight of species i, kg/mol
r = radial coordinate, m
R = radius of the gas–polymer interface, m
t = time, s
V = carrier gas velocity, m/s
V_0 = characteristic carrier gas velocity, m/s
z = axial coordinate, m
τ = polymer coating thickness, m
$\alpha_{ij} = R/K_{pij}\tau$ = thermodynamic dimensionless group
$\beta_{ij}^2 = V_0\tau^2/LD_{pij}$ = polymer-phase diffusion dimensionless group
$\gamma_{ij} = D_{gij}/LV_0$ = axial dispersion dimensionless group
$\lambda = C_{01}/C_{02}$ = ratio of the inlet pulse strengths

Literature Cited

1. Macris A. *Measurement of Diffusion and Thermodynamic Interactions in Polymer–Solvent Systems Using Capillary Column Inverse Gas Chromatography*. PhD Thesis. Amherst, MA: Dept. of Chemical Engineering, University of Massachusetts; 1979.
2. Pawlisch CA, Laurence RL, Macris A. Solute diffusion in polymers. 1. The use of capillary column inverse gas chromatography. *Macromolecules.* 1988;20:1564.
3. Arnould DD. *Capillary Column Inverse Gas Chromatography (CCIGC) for the Study of Diffusion in Polymer Solvent Systems*. PhD Thesis. Amherst, MA: Dept. of Chemical Engineering, University of Massachusetts; 1989.
4. Hadj Romdhane I. *Polymer–Solvent Diffusion and Equilibrium Parameters by Inverse Gas–Liquid Chromatography*. PhD Thesis. State College, PA: Dept. of Chemical Engineering, The Pennsylvania State University; 1994.
5. Danner RP, Tihminlioglu F, Surana RK, Duda JL. Inverse gas chromatography applications in polymer–solvent systems. *Fluid Phase Equilibria.* 1998;148:171.
6. Joffrion LL, Glover CJ. Vapor–liquid equilibrium of the ternary *n*-

heptane/isopropyl alcohol/atactic polypropylene mixture from perturbation gas chromatography. *Macromolecules.* 1986;19:1710.
7. Tsotsis TK, Turchi C, Glover CJ. Comparison of multi-component gas chromatography measurements of vapor–liquid equilibrium with static measurements using a polymer/two solvent ternary system. *Macromolecules.* 1987;20:2445.
8. Tanbonliong JO, Prausnitz JM. Vapour–liquid equilibria for some binary and ternary polymer solutions. *Polymer.* 1997;38:5775.
9. Liu H, Huang Y, Wang K, Hu Y. Vapor–liquid equilibria for mixed solvents–polymer systems: Measurement and correlation. *Fluid Phase Equilib.* 2002;194:1067.
10. Hong SU, Barbari TA, Sloan JM. Multicomponent diffusion of methyl ethyl ketone and toluene in polyisobutylene from vapor sorption FTIR-ATR spectroscopy. *J Polym Sci Part B: Polym Phys.* 1998;36:337.
11. Price PE, Wang S, Romdhane IH. Extracting effective diffusion parameters from drying experiments. *J Eng Appl Sci.* 1997;43:1925.
12. Alsoy S, Duda JL. Modeling of multicomponent drying of polymer films. *AIChE J.* 1999;45:896.
13. Zielinski JM, Hanley BF. Practical friction-based approach to modeling multicomponent diffusion. *AIChE J.* 1999;45:1.
14. Brockmeier NF, McCoy RW, Meyer JA. Gas chromatographic determination of thermodynamic properties of polymer solutions. I. Amorphous polymer systems. *Macromolecules.* 1972;5:464.
15. Brockmeier NF, McCoy RW, Meyer JA. Gas chromatographic determination of thermodynamic properties of polymer solutions. II. Semicrystalline polymer systems. *Macromolecules.* 1972;6:176.
16. Brockmeier NF, McCoy RW, Meyer JA. Gas chromatographic determination of thermodynamic properties of polymer solutions. *Macromolecules.* 1972;5:130.
17. Toor HL. Solution of the linearized equations of multicomponent mass transfer: I. *AIChE J.* 1964;10:448.
18. Kirkaldy JS, Weichert D, Zia-Ul-Haq. Diffusion in multicomponent metallic systems. VI. Some thermodynamic properties of the D matrix and the corresponding solutions of the diffusion equations. *Can J Phys.* 1963;41:2166.
19. Price PE, Romdhane IH. Multicomponent diffusion theory and its applications to polymer–solvent systems. *AIChE J.* 2003;49:309.
20. Surana RK, Danner RP, Tihminlioglu F, Duda JL. Evaluation of inverse gas chromatography for prediction and measurement of diffusion coefficients. *J Polym Sci Part B: Polym Phys.* 1997;35:1233.
21. Surana RK. *Advances in Diffusion and Partition Measurements in Polymer–Solvent Systems Using Inverse Gas Chromatography*. PhD Thesis. State College, PA: Dept. of Chemical Engineering, The Pennsylvania State University; 1997.
22. Vrentas JS, Vrentas CM, Hadj Romdhane I. Analysis of inverse gas chromatography experiments. *Macromolecules.* 1993;26:6670.

Appendix A: Model Solution

To aid in the model solution, the following dimensionless variables are introduced

$$\begin{bmatrix}\rho_1'\\ \rho_2'\end{bmatrix} = \begin{bmatrix}\dfrac{\rho_1-\rho_{1b}}{\dfrac{V_0}{L}K_{p11}C_{01}}\\ \dfrac{\rho_2-\rho_{2b}}{\dfrac{V_0}{L}K_{p22}C_{02}}\end{bmatrix} \tag{A1}$$

$$\begin{bmatrix}C_1'\\ C_2'\\ C_3'\end{bmatrix} = \begin{bmatrix}\dfrac{C_1-C_{b1}}{\dfrac{C_{01}V_0}{L}}\\ \dfrac{C_2-C_{b2}}{\dfrac{C_{02}V_0}{L}}\\ \dfrac{C_3-C_{b3}}{\dfrac{C_{03}V_0}{L}}\end{bmatrix} \tag{A2}$$

$$t' = \frac{tV}{L} \tag{A3}$$

$$r' = \frac{r-R}{\tau} \tag{A4}$$

$$z' = \frac{z}{L} \tag{A5}$$

Here, V_0 is the characteristic carrier gas velocity. Substituting these variables into polymer species continuity equations (Eqs. 12–15) gives

$$\frac{\partial}{\partial t'}\begin{bmatrix}\rho_1'\\ \rho_2'\end{bmatrix} = \begin{bmatrix}\dfrac{1}{\beta_{11}^2} & \dfrac{\alpha_{11}}{\alpha_{22}\beta_{12}^2\lambda}\\ \dfrac{\alpha_{22}\lambda}{\alpha_{11}\beta_{21}^2} & \dfrac{1}{\beta_{22}^2}\end{bmatrix}\frac{\partial^2}{\partial r'^2}\begin{bmatrix}\rho_1'\\ \rho_2'\end{bmatrix} \tag{A6}$$

$$t' = 0 \qquad \begin{bmatrix}\rho_1'\\ \rho_2'\end{bmatrix} = \begin{bmatrix}0\\ 0\end{bmatrix} \tag{A7}$$

$$r' = 0 \qquad \begin{bmatrix}\rho_1'\\ \rho_2'\end{bmatrix} = \begin{bmatrix}1 & \dfrac{\alpha_{11}}{\alpha_{12}\lambda}\\ \dfrac{\alpha_{22}\lambda}{\alpha_{21}} & 1\end{bmatrix}\begin{bmatrix}C_1'\\ C_2'\end{bmatrix} \tag{A8}$$

$$r' = 1 \qquad \frac{\partial}{\partial r'}\begin{bmatrix}\rho_1'\\ \rho_2'\end{bmatrix} = \begin{bmatrix}0\\ 0\end{bmatrix} \tag{A9}$$

Summation of the three species continuity equations (Eqs. 6–8) for the gas phase gives the total continuity equation

$$C\frac{\partial V}{\partial z} = \frac{2}{R}\left(D_{p11}\frac{\partial \rho_1}{\partial r}\bigg|_{r=R} + D_{p12}\frac{\partial \rho_2}{\partial r}\bigg|_{r=R}\right) + \frac{2}{R}\left(D_{p21}\frac{\partial \rho_1}{\partial r}\bigg|_{r=R} + D_{p22}\frac{\partial \rho_2}{\partial r}\bigg|_{r=R}\right) \tag{A10}$$

Substituting the dimensionless variables into this equation gives

$$\frac{\partial V'}{\partial z'} = \frac{2}{\alpha_{11}\beta_{11}^2}\left(\frac{C_{01}V_0}{CL}\right)\frac{\partial \rho_1'}{\partial r'}\bigg|_{r'=0} + \frac{2}{\alpha_{22}\beta_{12}^2}\left(\frac{C_{02}V_0}{CL}\right)\frac{\partial \rho_2'}{\partial r'}\bigg|_{r'=0} + \frac{2}{\alpha_{11}\beta_{21}^2}\left(\frac{C_{01}V_0}{CL}\right)\frac{\partial \rho_1'}{\partial r'}\bigg|_{r'=0} + \frac{2}{\alpha_{22}\beta_{22}^2}\left(\frac{C_{02}V_0}{CL}\right)\frac{\partial \rho_2'}{\partial r'}\bigg|_{r'=0} \tag{A11}$$

For a typical CCIGC experiment, $(C_{0i}V_0/CL)$is on the order of 10^{-5}, whereas $2/\alpha_1\beta_{21}^2$ is usually on the order of 1 or 10. Thus, it can be safely assumed that the mass average velocity in the column is constant

$$\frac{\partial V'}{\partial z'} = 0 \qquad \text{and} \qquad V = V_0 \tag{A12}$$

Under this approximation, the solvent species continuity equations simplify to

$$\frac{\partial C_1}{\partial t} + V_0 \frac{\partial C_1}{\partial z} = D_{g11} \frac{\partial^2 C_1}{\partial z^2} + \frac{2}{R}\left(D_{p11} \frac{\partial \rho_1}{\partial r}\bigg|_{r=R} + D_{p12} \frac{\partial \rho_2}{\partial r}\bigg|_{r=R} \right) \tag{A13}$$

$$\frac{\partial C_2}{\partial t} + V_0 \frac{\partial C_2}{\partial z} = D_{g22} \frac{\partial^2 C_2}{\partial z^2} + \frac{2}{R}\left(D_{p21} \frac{\partial \rho_1}{\partial r}\bigg|_{r=R} + D_{p22} \frac{\partial \rho_2}{\partial r}\bigg|_{r=R} \right) \tag{A14}$$

Because the velocity is assumed constant, it is no longer necessary to consider the carrier gas continuity equation. The solvent species continuity equations can be expressed in dimensionless form

$$\frac{\partial}{\partial t'}\begin{bmatrix} C_1' \\ C_2' \end{bmatrix} + \frac{\partial}{\partial z'}\begin{bmatrix} C_1' \\ C_2' \end{bmatrix} = [\gamma] \frac{\partial^2}{\partial z'^2}\begin{bmatrix} C_1' \\ C_2' \end{bmatrix} + [D] \frac{\partial}{\partial r'}\begin{bmatrix} \rho_1' \\ \rho_2' \end{bmatrix}\bigg|_{r'=0} \tag{A15}$$

where

$$[D] = 2\begin{bmatrix} \dfrac{1}{\alpha_{11}\beta_{11}^2} & \dfrac{1}{\lambda\alpha_{22}\beta_{12}^2} \\ \dfrac{\lambda}{\alpha_{11}\beta_{21}^2} & \dfrac{1}{\alpha_{22}\beta_{22}^2} \end{bmatrix}$$

and

$$[\gamma] = \begin{bmatrix} \dfrac{D_{g11}}{V_0 L} & 0 \\ 0 & \dfrac{D_{g22}}{V_0 L} \end{bmatrix}$$

In dimensionless form, the necessary boundary conditions are

$$t' = 0 \qquad \begin{bmatrix} C_1' \\ C_2' \end{bmatrix} = \begin{bmatrix} 0 \\ 0 \end{bmatrix} \tag{A16}$$

$$z' = 0 \qquad \begin{bmatrix} C_1' \\ C_2' \end{bmatrix} = \begin{bmatrix} \delta(t') \\ \delta(t') \end{bmatrix} \tag{A17}$$

$$z' = \infty \qquad \begin{bmatrix} C_1' \\ C_2' \end{bmatrix} = \begin{bmatrix} 0 \\ 0 \end{bmatrix} \tag{A18}$$

Because dimensional analysis showed the gas velocity to be constant, the governing equations are linear. This makes an analytical solution possible. Macris[1] showed that the equations for the binary system can be solved using Laplace transforms. This approach cannot be directly applied because the equations are coupled. To uncouple the equations a new matrix, $[A]$, is defined. This matrix is constructed by setting its columns to the eigenvectors of the matrix in Eq. A6

$$[A] = \begin{bmatrix} 1 & \dfrac{\hat{\beta}_2 - \dfrac{1}{\beta_{22}^2}}{\dfrac{\alpha_{22}\lambda}{\alpha_{11}\beta_{21}^2}} \\ \dfrac{\hat{\beta}_1 - \dfrac{1}{\beta_{11}^2}}{\dfrac{\alpha_{11}}{\alpha_{22}\lambda\beta_{12}^2}} & 1 \end{bmatrix} \tag{A19}$$

Here, $\hat{\beta}_1$ and $\hat{\beta}_2$ are the eigenvalues of the matrix in Eq. A6. They can be found from the quadratic rule to be

$$\hat{\beta}_1 = \frac{1}{2}\{\text{tr} + \sqrt{(\text{tr})^2 - 4\det}\} \tag{A20}$$

$$\hat{\beta}_2 = \frac{1}{2}\{\text{tr} - \sqrt{(\text{tr})^2 - 4\det}\} \tag{A21}$$

Here tr is the trace of the matrix

$$\begin{bmatrix} \dfrac{1}{\beta_{11}^2} & \dfrac{\alpha_{11}}{\alpha_{22}\lambda\beta_{12}^2} \\ \dfrac{\alpha_{22}\lambda}{\alpha_{11}\beta_{21}^2} & \dfrac{1}{\beta_{22}^2} \end{bmatrix}$$

and det is the determinant of the matrix. The reason for creating the $[A]$ is that is has a unique mathematical property

$$[A]^{-1}\begin{bmatrix} \dfrac{1}{\beta_{11}^2} & \dfrac{\alpha_{11}}{\alpha_{22}\lambda\beta_{12}^2} \\ \dfrac{\alpha_{22}\lambda}{\alpha_{11}\beta_{21}^2} & \dfrac{1}{\beta_{22}^2} \end{bmatrix}[A] = \begin{bmatrix} \hat{\beta}_1 & 0 \\ 0 & \hat{\beta}_2 \end{bmatrix} \tag{A22}$$

Multiplying both sides of Eq. A6 by $[A]^{-1}$ gives

$$\frac{\partial}{\partial t'}[A]^{-1}\begin{bmatrix} \rho_1' \\ \rho_2' \end{bmatrix} = [A]^{-1}\begin{bmatrix} \dfrac{1}{\beta_{11}^2} & \dfrac{\alpha_{11}}{\alpha_{22}\lambda\beta_{12}^2} \\ \dfrac{\alpha_{22}\lambda}{\alpha_{11}\beta_{21}^2} & \dfrac{1}{\beta_{22}^2} \end{bmatrix}[A] \times [A]^{-1}\frac{\partial^2}{\partial r'^2}\begin{bmatrix} \rho_1' \\ \rho_2' \end{bmatrix} \tag{A23}$$

The identity matrix $[I] = [A][A]^{-1}$ has been inserted between the matrix and the second derivative. Substituting Eq. A22 into this result gives

$$\frac{\partial}{\partial t'}\begin{bmatrix}\hat{\rho}_1' \\ \hat{\rho}_2'\end{bmatrix} = \begin{bmatrix}\hat{\beta}_1 & 0 \\ 0 & \hat{\beta}_2\end{bmatrix}\frac{\partial^2}{\partial r'^2}\begin{bmatrix}\hat{\rho}_1' \\ \hat{\rho}_2'\end{bmatrix} \tag{A24}$$

In this equation, pseudoconcentrations have been introduced

$$\begin{bmatrix}\hat{\rho}_1' \\ \hat{\rho}_2'\end{bmatrix} = [A]^{-1}\begin{bmatrix}\rho_1' \\ \rho_2'\end{bmatrix} \tag{A25}$$

Equation A24 can be written as two uncoupled partial differential equations in terms of these pseudocompositions

$$\frac{\partial \hat{\rho}_1'}{\partial t'} = \hat{\beta}_1\frac{\partial^2 \hat{\rho}_1'}{\partial r'^2} \tag{A26}$$

$$\frac{\partial \hat{\rho}_2'}{\partial t'} = \hat{\beta}_2\frac{\partial^2 \hat{\rho}_2'}{\partial r'^2} \tag{A27}$$

The boundary conditions are also multiplied by $[A]^{-1}$ to give

$$t' = 0 \qquad \begin{bmatrix}\hat{\rho}_1' \\ \hat{\rho}_2'\end{bmatrix} = \begin{bmatrix}0 \\ 0\end{bmatrix} \tag{A28}$$

$$r' = 0 \qquad \begin{bmatrix}\hat{\rho}_1' \\ \hat{\rho}_2'\end{bmatrix} = [B]\begin{bmatrix}\hat{C}_1' \\ \hat{C}_2'\end{bmatrix} \tag{A29}$$

where

$$[B] = [A]^{-1}\begin{bmatrix}1 & \dfrac{\alpha_{11}}{\alpha_{12}\lambda} \\ \dfrac{\alpha_{22}\lambda}{\alpha_{21}} & 1\end{bmatrix}[A]$$

$$r' = 1 \qquad \frac{\partial}{\partial r'}\begin{bmatrix}\hat{\rho}_1' \\ \hat{\rho}_2'\end{bmatrix} = \begin{bmatrix}0 \\ 0\end{bmatrix} \tag{A30}$$

The polymer-phase species continuity equations are now two uncoupled differential equations. These types of equations can be solved using Laplace transforms. The following Laplace domain variables are introduced

$$\begin{bmatrix}Q_1(s, r') \\ Q_2(s, r')\end{bmatrix} = \begin{bmatrix}\hat{\rho}_1'(t', r') \\ \hat{\rho}_2'(t', r')\end{bmatrix} \tag{A31}$$

$$\begin{bmatrix}Y_1(s, z') \\ Y_2(s, z')\end{bmatrix} = \begin{bmatrix}\hat{C}_1'(t', z') \\ \hat{C}_2'(t', z')\end{bmatrix} \tag{A32}$$

Using these variables, Eqs. A26 and A27 can be transformed into the Laplace domain

$$Q_1 \cdot s - \hat{\rho}_1'(t' = 0) = \hat{\beta}_1\frac{\partial^2 Q_1}{\partial r'^2} \tag{A33}$$

$$Q_2 \cdot s - \hat{\rho}_2'(t' = 0) = \hat{\beta}_2\frac{\partial^2 Q_2}{\partial r'^2} \tag{A34}$$

Using the initial condition from Eq. A28

$$\frac{\partial^2 Q_1}{\partial r'^2} - \frac{Q_1 \cdot s}{\hat{\beta}_1} = 0 \tag{A35}$$

$$\frac{\partial^2 Q_2}{\partial r'^2} - \frac{Q_2 \cdot s}{\hat{\beta}_2} = 0 \tag{A36}$$

The boundary conditions are also transformed into the Laplace domain

$$r' = 0 \qquad \begin{bmatrix}Q_1 \\ Q_2\end{bmatrix} = [B]\begin{bmatrix}Y_1 \\ Y_2\end{bmatrix} \tag{A37}$$

$$r' = 1 \qquad \frac{\partial}{\partial r'}\begin{bmatrix}Q_1 \\ Q_2\end{bmatrix} = \begin{bmatrix}0 \\ 0\end{bmatrix} \tag{A38}$$

Equations A35 and A36 are second-order linear homogeneous equations with constant coefficients. Thus, the general solutions have the form

$$Q_1 = c_1 e^{\sqrt{s/\hat{\beta}_1}r'} + c_2 e^{-\sqrt{s/\hat{\beta}_2}r'} \tag{A39}$$

$$Q_2 = c_3 e^{\sqrt{s/\hat{\beta}_2}r'} + c_4 e^{-\sqrt{s/\hat{\beta}_2}r'} \tag{A40}$$

The c_i are constants that are determined from the boundary conditions given in Eqs. A37 and A38. With these constants, the solution reduces to

$$Q_1 = (B_{11}Y_1 + B_{12}Y_2) \times \left(\frac{1}{1 + e^{\sqrt[2]{s/\hat{\beta}_1}}}e^{\sqrt{s/\hat{\beta}_1}r'} + \frac{e^{\sqrt[2]{s/\hat{\beta}_1}}}{1 + e^{\sqrt[2]{s/\hat{\beta}_1}}}e^{-\sqrt{s/\hat{\beta}_1}r'}\right) \tag{A41}$$

$$Q_2 = (B_{21}Y_1 + B_{22}Y_2) \times \left(\frac{1}{1 + e^{\sqrt[2]{s/\hat{\beta}_2}}}e^{\sqrt{s/\hat{\beta}_2}r'} + \frac{e^{\sqrt[2]{s/\hat{\beta}_2}}}{1 + e^{\sqrt[2]{s/\hat{\beta}_2}}}e^{-\sqrt{s/\hat{\beta}_2}r'}\right) \tag{A42}$$

The gas-phase equation requires the gradient of Q_i at the gas–polymer interface. This is found by differentiating Eqs. A41 and A42 with respect to r'

$$\left(\frac{\partial}{\partial r'}\right)_{r'=0}\begin{bmatrix}Q_1 \\ Q_2\end{bmatrix} = [C]\begin{bmatrix}Y_1 \\ Y_2\end{bmatrix} \tag{A43}$$

where

$$[C] = \begin{bmatrix}-\sqrt{\dfrac{s}{\hat{\beta}_1}}\tanh\left(\sqrt{\dfrac{s}{\hat{\beta}_1}}\right) & 0 \\ 0 & -\sqrt{\dfrac{s}{\hat{\beta}_2}}\tanh\left(\sqrt{\dfrac{s}{\hat{\beta}_2}}\right)\end{bmatrix}[B]$$

As with the polymer phase, both sides of the gas-phase equations can be multiplied by $[A]^{-1}$

$$[A]^{-1}\frac{\partial}{\partial t'}\begin{bmatrix}C_1'\\C_2'\end{bmatrix}+[A]^{-1}\frac{\partial}{\partial z'}\begin{bmatrix}C_1'\\C_2'\end{bmatrix}=[A]^{-1}[\gamma][A][A]^{-1}\frac{\partial^2}{\partial z'^2}\begin{bmatrix}C_1'\\C_2'\end{bmatrix}+[A]^{-1}[D][A][A]^{-1}\frac{\partial}{\partial r'}\begin{bmatrix}\rho_1'\\\rho_2'\end{bmatrix}\Bigg|_{r'=0} \quad \text{(A44)}$$

It will be assumed that $D_{g11} = D_{g22}$. Although this is probably not a good approximation, the value of γ typically has an insignificant effect on the shape of the elution profile.[22] Thus, using this approximation should not affect the end result. With this assumption, $[\gamma]$ is a symmetric matrix, and Eq. A44 and the boundary conditions can be written as

$$\frac{\partial}{\partial t'}\begin{bmatrix}\hat{C}_1'\\\hat{C}_2'\end{bmatrix}+\frac{\partial}{\partial z'}\begin{bmatrix}\hat{C}_1'\\\hat{C}_2'\end{bmatrix}=[\gamma]\frac{\partial^2}{\partial z'^2}\begin{bmatrix}\hat{C}_1'\\\hat{C}_2'\end{bmatrix}+[E]\frac{\partial}{\partial r'}\begin{bmatrix}\hat{\rho}_1'\\\hat{\rho}_2'\end{bmatrix}\Bigg|_{r'=0} \quad \text{(A45)}$$

$$t'=0 \qquad \begin{bmatrix}\hat{C}_1'\\\hat{C}_2'\end{bmatrix}=\begin{bmatrix}0\\0\end{bmatrix} \quad \text{(A46)}$$

$$z'=0 \qquad \begin{bmatrix}\hat{C}_1'\\\hat{C}_2'\end{bmatrix}=[A]^{-1}\begin{bmatrix}\delta(t')\\\delta(t')\end{bmatrix} \quad \text{(A47)}$$

$$z'=\infty \qquad \begin{bmatrix}\hat{C}_1'\\\hat{C}_2'\end{bmatrix}=\begin{bmatrix}0\\0\end{bmatrix} \quad \text{(A48)}$$

In Eq. A45, $[E] = [A]^{-1}[D][A]$. Using the variables defined in Eqs. A31 and A32, these equations can be converted into the Laplace domain

$$s\begin{bmatrix}Y_1\\Y_2\end{bmatrix}+\frac{\partial}{\partial z'}\begin{bmatrix}Y_1\\Y_2\end{bmatrix}=[\gamma]\frac{\partial^2}{\partial z'^2}\begin{bmatrix}Y_1\\Y_2\end{bmatrix}+[E]\frac{\partial}{\partial r'}\begin{bmatrix}Q_1\\Q_2\end{bmatrix}\Bigg|_{r'=0} \quad \text{(A49)}$$

$$z'=0 \qquad \begin{bmatrix}Y_1\\Y_2\end{bmatrix}=[A]^{-1}\begin{bmatrix}1\\1\end{bmatrix} \quad \text{(A50)}$$

$$z'=\infty \qquad \begin{bmatrix}Y_1\\Y_2\end{bmatrix}=\begin{bmatrix}0\\0\end{bmatrix} \quad \text{(A51)}$$

Substituting for the gradient given by Eq. A43

$$s\begin{bmatrix}Y_1\\Y_2\end{bmatrix}+\frac{\partial}{\partial z'}\begin{bmatrix}Y_1\\Y_2\end{bmatrix}=[\gamma]\frac{\partial^2}{\partial z'^2}\begin{bmatrix}Y_1\\Y_2\end{bmatrix}+[F]\begin{bmatrix}Y_1\\Y_2\end{bmatrix} \quad \text{(A52)}$$

In this equation

$$[F]=[E]\begin{bmatrix}-\sqrt{\frac{s}{\hat{\beta}_1}}\tanh\left(\sqrt{\frac{s}{\hat{\beta}_1}}\right) & 0\\ 0 & -\sqrt{\frac{s}{\hat{\beta}_2}}\tanh\left(\sqrt{\frac{s}{\hat{\beta}_2}}\right)\end{bmatrix}[B]$$

Next, the equations must be uncoupled by multiplying both sides of the equation by another matrix, $[G]^{-1}$

$$s[G]^{-1}\begin{bmatrix}Y_1\\Y_2\end{bmatrix}+[G]^{-1}\frac{\partial}{\partial z'}\begin{bmatrix}Y_1\\Y_2\end{bmatrix}=[G]^{-1}[\gamma][G]\times[G]^{-1}\frac{\partial^2}{\partial z'^2}\begin{bmatrix}Y_1\\Y_2\end{bmatrix}+[G]^{-1}[F][G][G]^{-1}\begin{bmatrix}Y_1\\Y_2\end{bmatrix} \quad \text{(A53)}$$

Similar to $[A]$ for the polymer phase, $[G]$ is constructed from the eigenvectors of $[F]$

$$[G]=\begin{bmatrix}1 & \frac{\hat{F}_2-F_{22}}{F_{21}}\\ \frac{\hat{F}_1-F_{11}}{F_{12}} & 1\end{bmatrix} \quad \text{(A54)}$$

where $\hat{F}_1$ and $\hat{F}_2$ are the eigenvalues of the $[F]$ matrix. They can be found from the quadratic rule to be

$$\hat{F}_1=\frac{1}{2}\{\text{tr}+\sqrt{(\text{tr})^2-4\,\text{det}}\} \quad \text{(A55)}$$

$$\hat{F}_2=\frac{1}{2}\{\text{tr}-\sqrt{(\text{tr})^2-4\,\text{det}}\} \quad \text{(A56)}$$

Here tr is the trace of the F matrix and det is the determinant of the G matrix. The reason for creating the G matrix is that it has a unique mathematical property

$$[G]^{-1}[F][G]=\begin{bmatrix}\hat{F}_1 & 0\\ 0 & \hat{F}_2\end{bmatrix} \quad \text{(A57)}$$

Here, new pseudo-Laplace variables are defined:

$$\begin{bmatrix}\hat{Y}_1\\\hat{Y}_2\end{bmatrix}=[G]^{-1}\begin{bmatrix}Y_1\\Y_2\end{bmatrix} \quad \text{(A58)}$$

Substitution of these pseudovariables gives

$$s\begin{bmatrix}\hat{Y}_1\\\hat{Y}_2\end{bmatrix}+\frac{\partial}{\partial z'}\begin{bmatrix}\hat{Y}_1\\\hat{Y}_2\end{bmatrix}=[\gamma]\frac{\partial^2}{\partial z'^2}\begin{bmatrix}\hat{Y}_1\\\hat{Y}_2\end{bmatrix}+\begin{bmatrix}\hat{F}_1 & 0\\ 0 & \hat{F}_2\end{bmatrix}\begin{bmatrix}\hat{Y}_1\\\hat{Y}_2\end{bmatrix} \quad \text{(A59)}$$

$$z' = 0 \qquad \begin{bmatrix} \hat{Y}_1 \\ \hat{Y}_2 \end{bmatrix} = \begin{bmatrix} H_1 \\ H_2 \end{bmatrix} \tag{A60}$$

$$z' = \infty \qquad \begin{bmatrix} \hat{Y}_1 \\ \hat{Y}_2 \end{bmatrix} = \begin{bmatrix} 0 \\ 0 \end{bmatrix} \tag{A61}$$

In Eq. A60

$$\begin{bmatrix} H_1 \\ H_2 \end{bmatrix} = [G]^{-1}[A]^{-1} \begin{bmatrix} 1 \\ 1 \end{bmatrix}$$

The uncoupled equations can be written as

$$\frac{\partial^2 \hat{Y}_1}{\partial z'^2} - \frac{1}{\gamma_1}\frac{\partial \hat{Y}_1}{\partial z'} - \psi_1(s)\hat{Y}_1 = 0 \tag{A62}$$

$$\frac{\partial^2 \hat{Y}_2}{\partial z'^2} - \frac{1}{\gamma_2}\frac{\partial \hat{Y}_2}{\partial z'} - \psi_2(s)\hat{Y}_2 = 0 \tag{A63}$$

where

$$\psi_i(s) = \frac{s - \hat{F}_i}{\gamma_i}$$

Like the polymer-phase equations, these are second-order linear homogeneous differential equations with constant coefficients. Thus, the general solutions have the form

$$\hat{Y}_1 = c_1 \exp\left\{z'\left(\frac{1}{2\gamma_1} + \sqrt{\frac{1}{4\gamma_1^2} + \psi_1(s)}\right)\right\} + c_2 \exp\left\{z'\left(\frac{1}{2\gamma_1} - \sqrt{\frac{1}{4\gamma_1^2} + \psi_1(s)}\right)\right\} \tag{A64}$$

$$\hat{Y}_2 = c_3 \exp\left\{z'\left(\frac{1}{2\gamma_2} + \sqrt{\frac{1}{4\gamma_2^2} + \psi_2(s)}\right)\right\} + c_4 \exp\left\{z'\left(\frac{1}{2\gamma_2} - \sqrt{\frac{1}{4\gamma_2^2} + \psi_2(s)}\right)\right\} \tag{A65}$$

Here, c_i are constants that can be determined from the boundary conditions. Using Eqs. A60 and A61, the general solution is found to be

$$\hat{Y}_i = H_i \exp\left\{z'\left(\frac{1}{2\gamma_i} - \sqrt{\frac{1}{4\gamma_i^2} + \psi_i(s)}\right)\right\} \tag{A66}$$

Because the gas concentration at the detector is needed, this expression is evaluated at the end of the column ($z' = 1$).

$$\hat{Y}_i = H_i \exp\left\{\frac{1}{2\gamma_i} - \sqrt{\frac{1}{4\gamma_i^2} + \psi_i(s)}\right\} \tag{A67}$$

Appendix B. Details of Numerical Solution

The numerical model is based on an implicit finite-difference technique. First, the species continuity equations for the gas and polymer phases are discretized using a Taylor series expansion. For example, the polymer-phase solvent 1 continuity equation given in Eq. A6 is expressed as

$$\frac{\rho'_{1,i} - \rho'_{1,i-1}}{\Delta t} = \frac{1}{\beta_{11}^2}\left(\frac{\rho'_{1,j+1} - 2\rho'_{1,j} + \rho'_{1,j-1}}{\Delta r^2}\right) + \frac{\alpha_{11}}{\alpha_{22}\beta_{12}^2\lambda}\left(\frac{\rho'_{2,j+1} - 2\rho'_{2,j} + \rho'_{2,j-1}}{\Delta r^2}\right) \tag{B1}$$

Here, the i and j subscripts represent discretized time and radial positions, Δt and Δr are the sizes of the time and radial step, respectively. A similar equation can be derived for solvent 2. The discretized gas-phase continuity equation for solvent 1 is

$$\frac{C'_{1,i} - C'_{1,i-1}}{\Delta t} + \frac{C'_{1,k} - C'_{1,k-1}}{\Delta z} = \gamma_1\left(\frac{C'_{1,k+1} - 2C'_{1,k} + C'_{1,k-1}}{\Delta z^2}\right) + D_{11}\left(\frac{\rho'_{1,j=2} - \rho'_{1,j=1}}{\Delta r}\right) + D_{12}\left(\frac{\rho'_{2,j=2} - \rho'_{2,j=1}}{\Delta r}\right) \tag{B2}$$

Here, k represents the discrete axial positions in the column and Δz is the axial step size. An expression similar to Eq. B2 can be derived for solvent 2. The discretized polymer-phase boundary conditions are

$$t' = 0 \qquad \begin{bmatrix} \rho'_{1,j} \\ \rho'_{2,j} \end{bmatrix} = \begin{bmatrix} 0 \\ 0 \end{bmatrix} \tag{B3}$$

$$r' = 0 \qquad \begin{bmatrix} \rho'_{1,j=1,k} \\ \rho'_{2,j=1,k} \end{bmatrix} = \begin{bmatrix} 1 & \frac{\alpha_{11}}{\alpha_{12}\lambda} \\ \frac{\alpha_{22}\lambda}{\alpha_{21}} & 1 \end{bmatrix} \begin{bmatrix} C'_{1,k} \\ C'_{2,k} \end{bmatrix} \tag{B4}$$

$$r' = 1 \qquad \begin{bmatrix} \rho'_{1,j=N} \\ \rho'_{2,j=N} \end{bmatrix} = \begin{bmatrix} \rho'_{1,j=N-1} \\ \rho'_{2,j=N-1} \end{bmatrix} \tag{B5}$$

Here, N is the total number of discrete points in the radial direction. Similarly, the gas-phase boundary conditions are

$$t' = 0 \qquad \begin{bmatrix} C'_{1,k} \\ C'_{2,k} \end{bmatrix} = \begin{bmatrix} 0 \\ 0 \end{bmatrix} \tag{B6}$$

$$z' = 0 \qquad \begin{bmatrix} C'_{1,k=1} \\ C'_{2,k=1} \end{bmatrix} = \begin{bmatrix} \dfrac{1}{\Delta t} \\ \dfrac{1}{\Delta t} \end{bmatrix} \tag{B7}$$

$$z' = \infty \qquad \begin{bmatrix} C'_{1,k=10M} \\ C'_{2,k=10M} \end{bmatrix} = \begin{bmatrix} 0 \\ 0 \end{bmatrix} \tag{B8}$$

Here, M is the total number of discrete points in the axial direction. The condition at infinite z' was specified at a large value of z' ($k = 10M$). The gas- and polymer-phase species continuity equations were solved with a simple tridiagonal solver at each time step. A constant step size time integrator was used to solve all four equations at each time step in a marching fashion.

Manuscript received Aug. 18, 2003, and revision received Mar. 7, 2005.